Science Press

ARTICLE

Inhibitive Effect of NO₃⁻ on the Corrosion Behavior of U-0.79wt%Ti Alloy in NaCl Solution

Cai Dingzhou,   Chen Xianglin,   Wu Haoxi,   Wang Ming,   Yang Shanli,   Sang Ge,

Li Yingru

Materials Institution, China Academy of Engineering Physics, Mianyang 621700, China

Abstract: The inhibitive effect of NO_3^- on the corrosion behavior of U-0.79wt%Ti alloy in 0.01 mol/L NaCl solution was studied by electrochemical methods. The results show that NO_3^- ions possess inhibitive effect on the corrosion of U-0.79wt%Ti alloy in the solution containing Cl^- ions, which has a close relationship with the concentration of NO_3^-. When the concentration ratio of NO_3^- and Cl^- exceeds 0.1, NO_3^- could inhibit the appearance of the pitting on U-0.79 wt%Ti alloy effectively; however, when the ratio is less than 0.1, NO_3^- shows hardly any inhibitive effect on the corrosion behavior of U-0.79 wt%Ti alloy. In the viewpoint of electrochemical process, the NO_3^- could increase the open circuit potential (OCP) of the alloy and lower the concentration polarization; meanwhile, it could increase the limited diffusion current density. At the same time, NO_3^- could also lower the rate of active anode dissolution, and increase the pitting corrosion potential of U-0.79 wt%Ti alloy. The surface scratches experiments show that the inhibitive effect of NO_3^- may root from that the NO_3^- ions have precedence over Cl^- ions in being absorbed at the surface defects, which would inhibit the nucleation of pitting corrosion.

Key words: U-Ti alloy; NO_3^-; inhibitive effect; corrosion

Uranium has been widely applied as an important energy material for decades [1-4]. However, its high chemical reactivity makes metallic uranium easy to corrode when exposing to atmosphere environment, decreasing the performance together with its lifetime, which greatly restricts the applications of metallic uranium [5-7]. Thus, alloying with molybdenum, niobium, titanium, zirconium, etc., is widely applied to improve uranium's anticorrosion properties as well as mechanical properties. Among these uranium alloys, uranium-titanium alloy shows special advantages and attracts much attention for significantly improving the anticorrosion properties and mechanical properties by adding a small amount of alloy constituent (usually less than 1 wt%) [8,9]. Nevertheless, in the moist circumstance containing Cl^-, uranium-titanium alloy would still suffer severe corrosion [10,11].

Uranium could react with different kinds of matters in the natural environment, resulting in a complex oxidation corrosion process of metallic uranium or uranium alloy. NO_3^- is one of the commonest anions in the natural environment, possessing notable effects on oxidation behavior of metals' surfaces. Pyun et al [12] studied the inhibitive effect of NO_3^- on the pure Al's pitting corrosion in 0.1 mol/L NaCl solution, and they found that NO_3^- could diffuse into the oxidation layer of pure Al's surface and anchor with the oxide, suppressing the sensitivity of pure Al's pitting corrosion. Rehim et al [13] found that in the basic condition, there are competitive adsorptions between NO_3^- and OH^- on the Pb's surface; when NO_3^- ions occupy the adsorption positions and pass into the oxidation layer, they would promote the anodic dissolution of PbO in the oxidation layer, result-

ing in the destruction of the passive layer. By applying the EDX technique, Amin[14] found that nitrogen exists in the passive layer of metallic Zn formed in the neutral $NaNO_3$ solution, implying that NO_3^- could diffuse into the passive layer to promote the transformation from ZnO or $Zn(OH)_2$ to soluble $Zn(NO_3)_2$. From the above, it can be concluded that the interaction mechanism between NO_3^- and metals depends on the kind of metal and the environmental conditions. In this research, we evaluated the influences of NO_3^- on the corrosion behaviors of U-0.79wt%Ti alloy (U-0.79Ti in short, containing 0.79% Ti and more than 99% U in mass percentage) in the aqueous solutions containing Cl^- by an electrochemical method together with a scratch experiment, and discussed the inhibitive mechanism of NO_3^- on the pitting corrosion behavior of U-0.79Ti alloy.

1   Experiment

The samples were round shaped with a dimension of $\Phi 12$ mm×3 mm, cut from a U-0.79Ti ingot prepared by arc melting. Then the samples were maintained at 800 °C for 2 h in a vacuum oven, followed by quenching in ice water. The surface of the quenched samples was polished in a step-wise manner to 1200# grit with metallographic sandpaper, and washed by deionized water succeeded by ethanol. After drying in cold wind, the samples were finally prepared. To evaluate the inhibitive influences of NO_3^- on the pitting corrosion, scratches were made on the surface of the polished samples by a knife. $NaNO_3$ (AR) and NaCl (AR) were purchased from Aladdin.

All the electrochemical tests were conducted by 3-electrode system. The as-prepared samples were the working electrodes; saturated calomel electrode (SCE) was the reference electrode; Pt net with an area of 2 cm^2 was the counter electrode. The testing platform was the electrochemical working station CS2350 produced by Wuhan Corrtest Instrument Co. Ltd.

The samples were first immersed in the certain solution until the open-circuit potential reached a stable value, and then the electrochemical tests were conducted. The cathode polarization potential range was from −1.0 V (vs SCE) to 0 V (vs OCP, open circuit potential); the anode polarization beginning potential was 0 V (vs OCP), and the polarization was conducted until the current density reached 1 mA/cm^2. The swap rates of both polarizations were 1 mV/s. The electrochemical impedance spectroscopy (EIS) analysis was performed under the open-circuit potential, with the potential fluctuation of 10 mV and the swapping frequency range from 10^{-2} to 10^4 Hz.

The morphology of samples with scratches were studied by laser scanning confocal microscope (LEXT OLS4000, Japan). The surface oxide composition was studied by X-ray diffractometer (PHI-5600 ESCA, Holland) and XploRA Laser Raman Spectrometer (HORIBA JobinYvon, France).

2   Results and Discussion

2.1   Effects of NO_3^- on OCP

The change of the OCP could reflect the formation process of oxidation layer on the electrode's surface, and the change rate of OCP qualitatively reflects the formation rate of oxidation layer. Generally speaking, the more quickly the potential increases, the faster the oxidation layer forms. If the OCP decreases suddenly during the increase, it suggests that destructions occur to the oxidation layer during the immerse process; in other words, corrosive dissolution happens. In order to avoid the systemic errors brought by the differences between samples, all the electrochemical tests in this paper were conducted using one same sample with repeated polishing. The open-circuit potential changes of U-0.79Ti alloy in the solutions with different concentration ratios of $NaNO_3$ and NaCl for 40 min are illustrated in Fig.1. All the curves increase fast at the early stage in parabola-shapes, and   then increase slowly and linearly after about 750 s, no matter whether the solutions contain NO_3^- or not. These results indicate that U-0.79Ti alloy could form an oxidation layer with a certain thickness on the surface rapidly during the immerse process to protect the alloy matrix, since the open-circuit potentials have a close relationship with the formation process of oxidation layer. The addition of $NaNO_3$ in NaCl solutions could make the OCP higher than that in the simple 0.01 mol/L NaCl solution, while still lower than that in simple 0.1 mol/L $NaNO_3$ solution for the same immersing time. The reason why the addition of NO_3^- increases OCP may lie in that NO_3^- could enhance the thickness or compactness of the oxidation layer, and this is requiring further analysis, which is shown below.

2.2   Effects of NO_3^- on the cathode process

The cathode polarization curves of U-0.79Ti alloy in the solutions with different concentration ratios of $NaNO_3$ and NaCl are shown in Fig.2. All the curves could be divided into four regions: hydrogen evolution region (−1.0~−0.9 V,
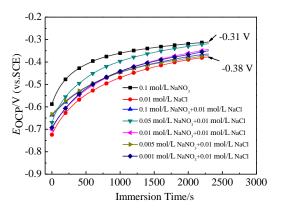

Fig.1   Open-circuit potentials of U-0.79Ti alloy in the solutions

with different concentration ratios of NaNO$_3$ and NaCl vs. SCE), concentration polarization region (−0.9 ~ −0.7 V, vs. SCE), strong polarization region (Tafel region, zero-current potential ±200 mV) and weak polarization region (zero-current potential ±50 mV). Here, it should be pointed out that the potential ranges above of the four regions in cathode polarization process are reference values, and the real potential ranges have small differences. Moreover, influenced by the scan rate and the cathode reduction process, zero-current potentials are usually lower than corresponding open-circuit potentials.

Usually, the cathode process of U-0.79Ti alloy in 0.01 mol/L NaCl solution contains two electrode reactions below:

$$2H^+ + 2e \rightarrow H_2 \tag{1}$$
$$O_2 + 2H_2O + 4e \rightarrow 4OH^- \tag{2}$$

In neutral conditions, the reduction reaction of oxygen (2) is considered to be the main reaction[15]. Although the U-0.79Ti alloy could form an oxidation layer (the main constituent is UO$_2$) with a certain thickness during the immerse process [16,17], no reduction reactions (except for oxygen reduction) would occur to the oxidation layer during the cathode polarization process[18], since the reduction potential of oxide layer is lower than the potential of hydrogen evolution at pH 7.0 (−0.85 V and −0.35 V relative to the standard hydrogen electrode, respectively, according to the Pourbaix diagram for uranium[19]). After adding NaNO$_3$, because of the relatively strong oxidability of NO$_3^-$, the cathode process would involve the reduction of NO$_3^-$ (3) [20].

$$NO_3^- + H_2O + 2e \rightarrow NO_2^- + 2OH^- \tag{3}$$

When the cathode polarization potential is relatively negative, in the hydrogen evolution region, the current densities of U-0.79Ti alloy in the solutions with NO$_3^-$ are larger than that in the solution without NO$_3^-$ due to the contribution of the reduction of NO$_3^-$. When the cathode polarization potential is in the concentration polarization region, the
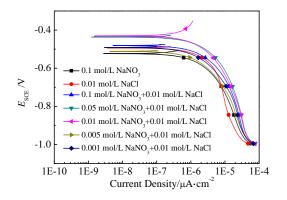
current density changes little with the potential, caused by the hybrid control of diffusion and reduction of dissolved oxygen. Meanwhile, the introduction of NO$_3^-$ makes the limited diffusion current density increase (Table 1), probably caused by the reduction of NO$_3^-$ during the cathode polarization process. Thus, it could be concluded that the cathode process is mainly influenced by the oxygen depolarization reaction and reduction of NO$_3^-$. Based on the electrode reaction (2) and (3), they could both make the pH increase at the interface of electrode reaction. As the U^{4+} could combine with OH$^-$ and transform into insoluble UO$_2$ 2H$_2$O or U(OH)$_4$) [21], the introduction of NO$_3^-$ into solution containing Cl$^-$ would inhibit the active dissolution of uranium in the alloy, improving the anti-corrosion properties of U-0.79Ti alloy.

Oxygen depolarization is a 4-electron reaction based on electrode reaction (2), which is more complex than hydrogen depolarization. Up to now, there is still not an agreed opinion on the oxygen depolarization, and it is roughly classified into two kinds of mechanisms in neutral solutions. The first kind of oxygen reduction mechanism is shown below[22]:

(1) Forming superoxide ions
$$O_2 + e \rightarrow O_2^- \tag{4}$$
(2) Forming HO$_2^-$ ions
$$O_2^- + H_2O + \rightarrow HO_2^- + OH^- \tag{5}$$
(3) Forming OH$^-$ ions
$$HO_2^- + H_2O + 2e \rightarrow 3OH^- \tag{6}$$
$$\text{Or } HO_2^- \rightarrow 1/2 \ O_2 + OH^- \tag{7}$$

Typically, the second step of receiving one electron (5) is considered to be the controlling step of oxygen depolarization among the above elementary reactions.

The second kind of mechanism holds that no HO$_2^-$ ion is produced during the ionization of oxygen, while absorbed oxygen or/and metal oxide on the surface should be the intermediate products. The elementary reactions are shown below [22]:

$$O_2 + 2M \rightarrow 2M-O \tag{8}$$

Table 1 Limited diffusion current densities of U-0.79Ti alloy in different test solutions

Test solutions	Limited diffusion current density/μA·cm^{-2}
0.1 mol/L NaNO$_3$	14.8
0.01 mol/L NaCl	10.7
0.1 mol/L NaNO$_3$ + 0.01 mol/L NaCl	21.9
0.05 mol/L NaNO$_3$ + 0.01 mol/L NaCl	26
0.01 mol/L NaNO$_3$ + 0.01 mol/L NaCl	24.8
0.005 mol/L NaNO$_3$ + 0.01 mol/L NaCl	17.3
0.001 mol/L NaNO$_3$ + 0.01 mol/L NaCl	20.2

Fig.2 Cathode polarization curves of U-0.79Ti alloy in the solutions with different concentration ratios of NaNO$_3$ and NaCl

$$M-O+2H_2O+2M(e)\rightarrow 2HO^-+3M \qquad (9)$$

Most of the redox reactions on the metal electrodes are considered to proceed according to the first mechanism. Also, as the uranium in the U-0.79Ti alloy possesses high chemical reactivity, the uranium oxide on the surface could exist stably, and is difficult to transfer into metallic uranium as the intermediate products. Thus, the reduction mechanism of oxygen on the surface of U-0.79Ti alloy is considered to be the first one discussed above in this paper.

When the cathode polarization potential increases continuously, the cathode process turns into the strong polarization region (i. e. the Tafel region), and the log of cathode polarization current density and the polarization potential follow the Tafel relationship. When the potential increases further into the weak polarization region, the cathode polarization current density and the polarization potential possess a linear relationship, showing that the reaction is electrochemically controlled.

2.3 Effects of NO_3^- on the anode process

As the anode oxidizing process of metallic uranium in aqueous solution consists of hydrolysis, and there are kinds of uranium species with different valences generated, it is more complex than the cathode process [23]. In this paper, we focus on the influences of NO_3^- on the pitting potential (E_{pit}, also known as oxide film destruction potential) and the cathode current density of U-0.79Ti alloy. The dissolving mechanism of uranium during the cathode process would be discussed in our future work. The anode polarization curves of U-0.79Ti alloy in the solutions with different concentration ratios of $NaNO_3$ and NaCl are shown in Fig.3. No matter whether the solution contains Cl^- or not, the corresponding curve shows no obvious passive region during the anode process. However, the E_{pit} (the potential when the current density reaches 100 $\mu A/cm^2$) in the simple 0.1 mol/L $NaNO_3$ solution is the highest among all the solutions. Also, during the anode processes in the solutions containing Cl^-, there are significant pitting potentials at which the current densities increase suddenly. Usually, the anode process mainly consists of the dissolution and repair of the oxide film on the alloy surface, following the reactions (10) and (11). When the oxide film destructs partially, i. e., the anode potential is higher than E_{pit}, the transformation from UO_2 to dissolvable UO_2^{2+} would be accelerated, resulting in sever pitting corrosion on the alloy surface.

$$U+O_2\rightarrow UO_2 \qquad (10)$$
$$UO_2\rightarrow UO_2^{2+}+2e \qquad (11)$$

Under the same anode polarization potential of -0.1 V (vs. SCE), if the concentration of NO_3^- exceeds 0.001 mol/L, the corresponding anode current densities are all lower than that in simple 0.01 mol/L NaCl solution; yet if the concentration of NO_3^- is 0.001 mol/L, the corresponding anode current density shows no obvious difference compared with
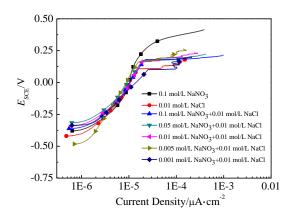

Fig.3   Anode polarization curves of U-0.79Ti alloy in the solutions with different concentration ratio of $NaNO_3$ and NaCl

that in simple 0.01 mol/L NaCl solution (Fig.4). These results imply that too low concentration of NO_3^- would have no obvious inhibitive influences on the anode dissolution of U-0.79Ti alloy in the aqueous solution containing Cl^-. Cl^-, NO_3^- and dissolved oxygen in the solution have a competitive adsorption relationship on the electrode surface, which leads to the differences of anode oxidization rate of U-0.79Ti alloy in different solutions; moreover, OH^- produced during the reduction of NO_3^- would inhibit the dissolution of the oxide film, which should be the reason that addition of a certain amount of $NaNO_3$ into the aqueous solution containing Cl^- would make anode current density of U-0.79Ti alloy decrease. However, the current densities changes and the concentrations of NO_3^- do not show a clear functional relationship, meaning the clear influences of NO_3^- still need further researches.
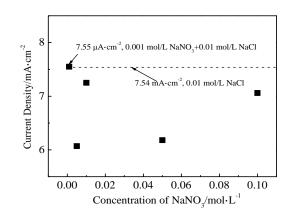

Fig.4   Anode current densities of U-0.79Ti alloy under the same anode polarization potential (-0.1 V) in the solutions with different concentration ratios of $NaNO_3$ and NaCl (the dash line is the anode current density in the solution without $NaNO_3$)
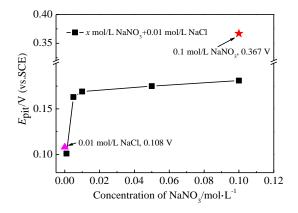
Fig.5   Pitting potentials of U-0.79Ti alloy in the solutions with different concentration ratios of NaNO₃ and NaCl

Based on the curves of anode polarization in Fig.3, the pitting corrosion potentials of U-0.79Ti alloy in the solutions with different concentration ratios of NaNO₃ and NaCl could be calculated (Fig.5). When the concentration of NaNO₃ in 0.01 mol/L NaCl solution is lower than 0.001 mol/L, the pitting corrosion potentials of U-0.79Ti alloy show no obvious differences compared with that in simple NaCl solution without NaNO₃. While when the concentration of NaNO₃ is higher than 0.001 mol/L, the pitting corrosion potentials of U-0.79Ti alloy would be increased significantly. However, even if the NaCl solution contain a plenty of NaNO₃, the pitting corrosion potential is still lower than that in simple NaNO₃ solution. These results indicate that Cl⁻ could obviously lower the pitting corrosion potential of U-0.79Ti alloy, while the NO₃⁻ could efficiently inhibit the corrosive effect of Cl⁻.

2.4   EIS analysis

The EIS plots give more details about the corrosion processes in different solutions. In the whole testing frequency range, the EIS plots of U-0.79Ti in different solutions show a single capacitive reactance arc, indicating all the electrode processes are controlled by electrode reactions (Fig.6a). The radius of the capacitive reactance arc in 0.1 mol/L NaNO₃ solution is significantly larger than that in 0.01 mol/L NaCl solution. Moreover, adding a certain amount of NaNO₃ in 0.01 mol/L NaCl solution could significantly increase the radius of capacitive reactance arc. In the Bode phase-plots (Fig.6b), all the plots of U-0.79Ti alloy in different solutions just show one time constant, probably determined by the thickness and/or compactness of the oxide membrane. Moreover, the difference of the time constants reflects that NO₃⁻ have influences on the thickness and/or compactness of the oxide membrane. In the Bode module-plots (Fig. 6b), the impedance modules of the U-0.79Ti samples in 0.1 mol/L NaNO₃ solution and
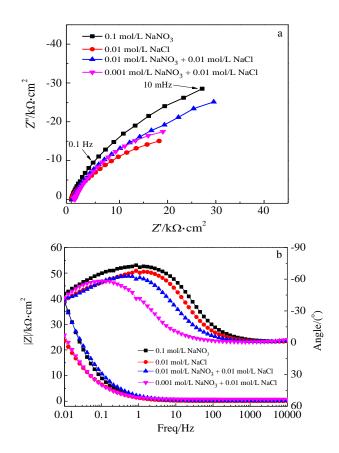

Fig.6   EIS of U-0.79Ti alloy in different solutions: (a) Nyquist plots and (b) Bode plots

0.01 mol/L NaNO₃ + 0.01 mol/L NaCl solution are obviously higher than those of the U-0.79Ti samples in 0.001 mol/L NaNO₃ + 0.01 mol/L NaCl solution and 0.01 mol/L NaCl solution. All these results above suggest that enough NO₃⁻ could inhibit the pitting corrosion in the solutions containing Cl⁻, while low concentration of NO₃⁻ does not possess this ability.

2.5   Inhibition effects of NO₃⁻ on the pitting corrosion

In order to study the inhibition effects of NO₃⁻ on the pitting corrosion of U-0.79Ti alloy visually, we made two scratches on both two samples manually with a knife. Then the two samples were separately immersed into 0.01 mol/L NaCl solution with or without 0.1 mol/L NO₃⁻ for 4 h. The morphologies were compared with the laser scanning confocal microscope (Fig.7). After immersing in the solutions without NO₃⁻ for 4 h, there are severe corrosion pits observed at the scratch positions. Also, there are corrosion spots at other areas. These results indicate that Cl⁻ possesses strong corrosive effect on the uranium-titanium alloy (Fig.7a~7c). On the contrary, after immersing in the solutions with 0.1 mol/L NO₃⁻ for 4 h, no obvious corrosion pits
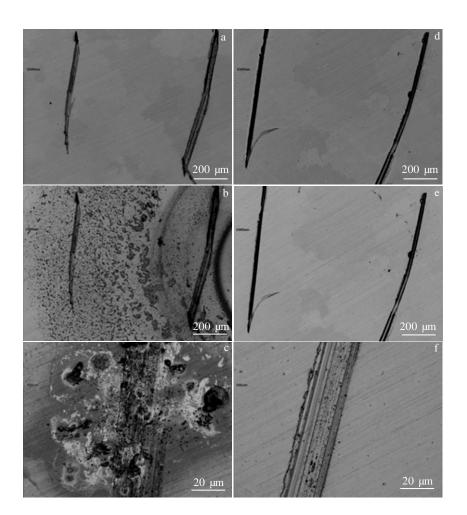
Fig.7   Optical morphologies of U-0.79Ti alloy immersed in different solutions for 4 h: (a) before immersing in 0.01 mol/L NaCl solution,
(b, c) after immersing in 0.01 mol/L NaCl solution; (d) before immersing in 0.1 mol/L $NaNO_3$ + 0.01 mol/L NaCl solution,
(e, f) after immersing in 0.1 mol/L $NaNO_3$ + 0.01 mol/L NaCl solution

appear at the scratch positions and no corrosion spots appear at other areas (Fig.7d~7f). These results directly exhibit that NO_3^- possess significant inhibition effect on the pitting corrosion of U-0.79Ti alloy in the solutions containing Cl^-. Based on the electrochemical analysis above, the inhibition effect should come from the completive adsorption, i. e., the NO_3^- ions are adsorbed in priority at the scratches which would inhibit the destruction of Cl^- on the oxidation layer.

The surface oxide species of the above samples immersed in different solutions were carefully studied by XRD and Raman spectra in order to fully comprehend the corrosion process and the influence of NO_3^-. The XRD patterns of both samples mainly show the existence of U and UO_2 (Fig.8), while the UO_2's characteristic peaks of the sample immersed in simple 0.1 mol/L NaCl solution is stronger than that of the sample immersed in 0.1 mol/L $NaNO_3$ + 0.01 mol/L NaCl solution, indicating the U-0.79Ti

alloy probably suffers severe corrosion. In other words, the NO_3^- could inhibit the corrosion in the environment containing Cl^-.

The Raman spectra give more information about the local distribution of uranium oxide on the surface. For the sample immersed in simple 0.01 mol/L NaCl solution, the Raman spectra of the regions where whether the pitting corrosion occurs (Site 1) or not (Site 2) shows obvious differences. Site 1 exhibits the characteristic peaks of U_3O_8, while Site 2 the characteristic peaks of UO_2 [24-26] (Fig.9a), implying that when the pitting corrosion occurs, it would lead the transformation from UO_2 to U_3O_8, which also confirm the generation of U(VI) during the pitting process immersed in simple NaCl solution, as the U_3O_8 is a kind of mixed-valence compound composed of UO_2 and UO_3 according the ratio of 1:2. According to the analysis above based on Fig.1 and Fig.3, the existence of Cl^- would decrease the open-circuit potential and the pitting corrosion
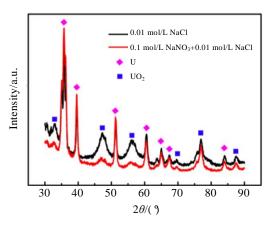
Fig.8　XRD patterns of U-0.79Ti alloy immersed in two different solutions 4 h

potential, suggesting the Cl^- could lower the activation energy from UO_2 to U_3O_8 as catalyst. However, for the sample immersed in the 0.1 mol/L $NaNO_3$ + 0.01 mol/L NaCl solution, the Raman spectra of the scratch region (Site 1) as well as the other regions (Site 2) shows only the characteristic peaks of UO_2 (Fig. 9b), which also confirms that sufficient NO_3^- could inhibit the catalytic effect of Cl^- and moreover the pitting corrosion of U-0.79Ti alloy in the solution containing Cl^-. At last, it also should be noted that
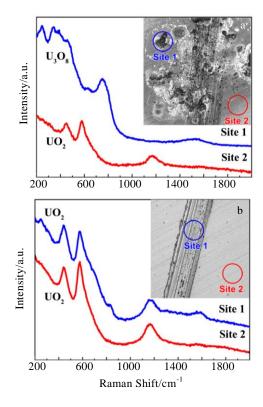

Fig.9　Raman spectra of different regions of U-0.79Ti alloy immersed in 0.01 mol/L NaCl solution (a) and 0.1 mol/L $NaNO_3$ + 0.01 mol/L NaCl solution (b)

due to the quite low content of titanium and its passive property, no obvious signals of titanium or titanium oxide were detected in either XRD or Raman spectra.

3　Conclusions

1) The introduction of NO_3^- into the aqueous solution containing Cl^- has influences on the whole electrochemical process. During the cathode process, NO_3^- could weaken the concentration polarization and increase the limited diffusion current density; while in the anode process, NO_3^- could increase the pitting corrosion potential of U-0.79Ti alloy and decrease the anode dissolving rate of the surface oxidation layer.

2) Moreover, only when the concentration ratio of NO_3^- and Cl^- is higher than 0.1, can NO_3^- possess the inhibition effect on the corrosion of U-0.79Ti in the aqueous solution containing Cl^-.

3) The scratch experiments prove that Cl^- could accelerate the pitting corrosion at the scratch position of U-0.79Ti alloy while NO_3^- could inhibit the pitting corrosion.

References

1　Wathen T. *Corrosion of Uranium Metal in Air and Steam at Various Temperatures,* No. BR-223A, R/GC/1304[R]. London: Imperial Chemical Industries, Ltd, 1943

2　Wilkinson W D. *Uranium Metallurgy: Uranium Corrosion and Alloys*[M]. New York: Interscience Publishers, 1962

3　Handley-Sidhu S, Bryan N D, Worsfold P J *et al. Chemosphere*[J], 2009, 77: 1434

4　Arkush R, Mintz M H, Shamir N. *J Nucl Mater*[J], 2000, 281: 182

5　Baker M M, Less L N, Orman S. *Trans Faraday Soc*[J], 1966, 62: 2513

6　Baker M M, Less L N, Orman S. *Trans Faraday Soc*[J], 1966, 62: 2525

7　Handleysidhu S, Keithroach M J, Lloyd J R *et al. Sci Total Environ*[J], 2010, 408: 5690

8　Greenholt C J, Weirick L J. *J Nucl Mater*[J], 1987, 144: 110

9　Shi P, Luo L Z, Zhao Y W *et al. Appl Surf Sci*[J], 2015, 343: 49

10　Cai D Z, Sang G, Wang Q F *et al. Rare Metal Mater Engineering* [J], 2014, 43: 1447 (in Chinese)

11　Cai D Z, Pan Q F, Li Y R *et al. Corrosion*[J], 2017, 73: 694

12　Pyun S I, Moon S M. *J Solid State Electrochem*[J], 1999, 3: 331

13　Rehim S S A E, Mohamed N F. *Corr Sci*[J], 1998, 40: 1883

14　Amin M A. *Electrochim Acta*[J], 2005, 50: 1265

15　Yang L T, Lu M X, Xin Q S. *Corrosion Monitoring Technique* [M]. Beijing: Chemical Industry Press, 2012 (in Chinese)

16　Ritchie A G. *J Nucl Mater*[J], 1981, 102: 170

17　Bloch J, Atzmony U, Dariel M P *et al. J Nucl Mater*[J], 1982, 105: 196

18　Burke J J. *Physical Metallurgy of Uranium Alloys*[M]. USA:

Hill Publishing Company, 1976

19 Wu W C. *Standard Electrode Potential Data Manual*[M]. Beijing: Science Press, 1991 (in Chinese)

20 Aramaki K, Shimura T. *Corr Sci*[J], 2011, 53: 4152

21 Rai D, Felmy A R, Ryan J L. *Inorganic Chem*[J], 1990, 21: 260

22 Wang F P. *Corrosion Electrochemical Principle, Method and Application*[M]. Beijing: Chemical Industry Press, 2015 (in Chinese)

23 Kim Y S. *J Nucl Mater*[J], 2000, 279: 173

24 Pointurier F, Marie O. *J Raman Spectroscopy*[J], 2014, 44: 1753

25 Lipp M J, Jenei Z, Klepeis J P *et al. Office of Scientific & Technical Information Technical Reports,* LLNL-TR-522251[R]. San Francisco: Lawrence Livermore National Laboratory, 2011

26 Manara D, Renker B. *J Nucl Mater*[J], 2003, 321: 233

硝酸根离子对 **U-0.79Ti** 合金腐蚀行为的抑制作用

蔡定洲，陈向林，吴昊曦，王　铭，杨善丽，桑　格，李英儒

(中国工程物理研究院材料研究所，四川 绵阳 621700)

摘　要：采用电化学方法研究了硝酸根离子（NO_3^-）对 U-0.79Ti 合金在 0.01 mol/L NaCl 溶液中腐蚀的抑制作用。实验证明，NO_3^-对 U-0.79Ti 合金在含氯离子（Cl^-）溶液中的腐蚀具有抑制作用，且与 NO_3^-浓度密切相关。当 NO_3^-与 Cl^-浓度比大于 0.1 时，NO_3^-能够有效抑制 U-0.79Ti 合金点蚀的发生；而低于这个比例时，NO_3^-对 U-0.79Ti 合金的腐蚀行为几乎无影响。从电化学过程来看，加入 NO_3^-能够降低浓差极化并增大极限扩散电流密度。同时，NO_3^-能够降低氧化膜的阳极活性溶解速度，提高 U-0.79Ti 合金的点蚀电位。表面划痕实验则表明，NO_3^-的抑制作用很可能缘于其优先于 Cl^-在表面缺陷处吸附，阻碍了 Cl^-的点蚀成核。

关键词：铀钛合金；硝酸根；抑制作用；腐蚀